A Hybrid Deep Learning Methodology for Breast Cancer Diagnosis using Magnetic Resonance Images

Seyyedreza Mirbagheri
Arak University

Maryam Momeni (m-momeni@araku.ac.ir)
Arak University

Research Article

Keywords: Breast Cancer, Deep Learning, Autoencoder, Magnetic Resonance Imaging, Convolution Neural Network

Posted Date: May 4th, 2022

DOI: https://doi.org/10.21203/rs.3.rs-1604535/v1

Abstract

Today, breast cancer is one of the most common causes of cancer in women. Precise diagnosis of cancerous tissues based on images is essential in disease treatment before the disease progression. Although there are several image techniques for diagnosing, magnetic resonance (MR) imaging contains extensive clinical information which usable with other image modalities such as mammography and ultrasound. In this study, the hybrid of an autoencoder network with ResNet architecture was proposed to significantly improve classification accuracy to diagnose breast cancer lesions into two categories: benign and malignant in MR images. Using the MR breast cancer images of the QIN-Breast database, the results present the employment of an autoencoder as a preprocessor can enhance the efficiency of CNN and ultimately lead to an accurate diagnosis of benign and malignant tissues by 97.65%. The proposed method significantly improved the classification from the point of view of speed, accuracy, and precision. This cancerous tissue classification was employed only using MR images without manual segmentation and feature extraction.

Introduction

According to the World Cancer Organization, one in eight women in the United States develops breast cancer [1], and it is generally the leading cause of death for women worldwide. By considering the latest figures released by the University of Oxford in 2017, breast cancer is the fifth leading cause of death globally, killing more than 600,000 people annually. Therefore, the accurate and early detection of cancerous tissues is critical. It can be very effective in quickly identifying malignant tumors as an initial step before the disease progress. Breast cancer has several symptoms like breast deformity, skin dimples, discharge of fluid from the nipple, or eczema of the epithelial tissue [2]. The diagnosis and treatment of breast cancer increase life expectancy in women. Therefore, finding diagnostic methods has a significant role in improving the patient's condition [3]. There are currently several ways for diagnosing this cancer, such as breast self-examination, mammography, and breast magnetic resonance (MR) images. MR imaging is a valuable diagnostic technique due to its high and acceptable sensitivity in dense breast tissues. This high-contrast MRI is very operative for the early detection of breast cancer in women at high risk of the disease. It detects the presence and spread of breast cancer in higher grades compared to mammography [4]. Additionally, MR images are a widespread and auxiliary clinical technique applicable with other imaging modalities like mammography and ultrasound [5, 6]. Breast cancer is one of the most common cancers studied by researchers using medical tests and imaging such as mammography, ultrasound, tomography [7–10]. On the other hand, deep learning (DL) networks perform well in diagnosis, especially in medical image processing. This study aimed to provide an intelligent method for differentiating breast cancer lesions into benign and malignant using the ability of DL networks to classify lesions with higher efficiency and better accuracy. Accordingly, after the literature review in the Section of Related Works, the MR images were utilized as inputs of autoencoder to have the images with more principal and accurate features. Thereafter, the reconstructed MR images of autoencoder were used as the inputs of CNN to classify the breast images into two groups of benign and malignant masses (the

Section of Method). Subsequently, the outcomes and the evaluations were reported in the Section of Experimental Results. Finally, the result analysis was done in the Section of Discussion and Conclusion.

Related Works

Some DL models and machine learning methods have been used to diagnose breast cancer types in the literature. Rakhlin et al., 2018 presented a method using a deep convolutional neural network (CNN) to analyze the histological image of breast cancer. By integrating several deep neural network architectures and optimized decision tree classification, the images have been classified into four groups with an accuracy of 87.2% [11]. Platania et al., 2017 presented a method called an automatic diagnosis of breast cancer using deep learning and diagnosis (BC-DROID), which provides an automated region of interest detection and diagnosis in mammography and MRI using CNN with the classification accuracy of 93.5%. To achieve higher accuracy, CNN was trained using the definite desired areas emerged by physicians. Then, the proposed system could classify the selected areas as benign or malignant in one step. To fast recognize breast cancer using neural networks, after the feature reduction by independent component analysis (ICA), the support vector machine (SVM) was utilized as a classifier. In addition to the higher efficiency of classification, the calculation cost decreased. Besides, the SVM performance compared to other classification methods like artificial neural networks (ANN), K-nearest neighbors (KNN), and radial basis function network (RBFN). The best performance was achieved when they utilized the RBFN with the classification accuracy of 90.49% using reduction features obtained of ICA [12]. Rasti et al., 2017, reported a novel computer-aided diagnosis (CAD) system in breast dynamic contrast-enhanced magnetic resonance imaging (DCE-MRI) [13]. The CAD system is designed based on a mixed ensemble of convolutional neural networks (ME-CNN) to diagnose benign and malignant tumors. Their proposed algorithm was a modular and image-based ensemble, which could stochastically partition the high-dimensional image space through simultaneous and competitive learning of its modules. The proposed system was assessed on our database of 112 DCE-MRI studies, including solid breast masses, using various classification measures. The ME-CNN model achieved an accuracy of 96.39%. Yurttakal et al., 2019 presented that CNN performance is better in image classification compared with feature-based methods. CNN was employed to diagnose lesions as malignant or benign tumors using MRI images. They achieved the accuracy classification of 98.33% using only pixel information and a multi-layer CNN architecture [14]. The deep-learning-based techniques were established for a doubtful region of interest (ROI) segmentation and classification using MRI modalities [15, 16].

Drukker et al., 2020 evaluated an extended short-term memory network to analyze breast cancer progression along with neoadjuvant chemotherapy at two and five years post-surgery. After the segmentation of breast cancers in MR images, the features related to the kinetic curves were extracted. The areas under the ROC curve in the prediction of this study at two years post-surgery were 0.80 [17]. Fusco et al., 2020 considered 45 patients subjected to DCE-MRI before and after the treatment. After extracting 11 semi-quantitative parameters and 50 texture features, the standardized shape index had the best results with a ROC-AUC of 0.93 to distinguish pathological response versus non-pathological response patients [18]. Elanthirayan et al., 2021 considered the breast MR slices to examine the breast

tumor section. They used a hybrid imaging procedure including Brain Storm Optimization Algorithm and Shannon's entropy thresholding and Active-Contour (AC) for tumor segmentation. The proposed experiment on 150 2D breast MRI slices yielded the average accuracy of AC (> 93%) [19]. Typically, lesion classification using DL-based methods is employed without precise segmentation. Antropova et al., 2016 implemented the combination of a pre-trained CNN with SVM to breast MR classification [20]. In addition to their results, other literature confirmed that fine-tuning all layers towards breast MRI classification are necessary to attain high performance [14, 16, 21–25].

Because of CNN training by RGB ImageNet images in grayscale, there are various methods based on the input to the pre-trained CNN like three-time points (3TP) method [22], precontrast, first postcontrast, and second postcontrast frames [17], DCE-MRI, T2-weighted MR, and diffusion-weighted image (DWI) [22, 23, 26]. Participating in both temporal and spatial features of breast MR is challenging for DL networks, especially for 2D images. In this regard, Antropova et al., 2018(a) employed maximum intensity projection (MIP) to incorporate spatial information, whereas image enhancement did not cause miss any evidence [27]. Hu et al., 2019 presented a pooling layer to reduce the image dimension at the feature level, instead of the image level, as in the MIP case [25]. Recurrent neural networks, such as long short-term memory (LSTM), were also practical for lesion classification [28–30]. In each ROI, morphological features extraction at different time points by a CNN were usable for LSTM training to predict the result based on the entire DCE-MRI sequence. Some proposed CNN architectures corresponding to the 4D nature of DCE-MRI by exploiting 3D convolutional layers [31–34] and by extracting unique features of DCE-MRI at multiple scales [32].

Method

As usual, the proposed method includes preprocessing, feature extraction, and classification. Although unsupervised neural networks usually do not require data preprocessing, the preprocessing of dataset images is necessary because of the variety of image acquisition systems with different quality and image protocols. Autoencoder networks play a crucial role in unsupervised deep networking, the autoencoders perform in two steps: coding and decoding. The outputs are reconstructed in the decoding step using the extracted salient features in the first coding stage. Then, the reconstructed images are enhanced with the reduced noises. Accordingly, in this study, the image quality was enhanced by an autoencoder to improve the CNN performance in data processing and classification. Thus, the obtained images of the autoencoder were used as the inputs of CNN in which the images were automatically parceled, and then the valuable features were extracted. According to the obtained features in the last layer of CNN, the images were classified into two groups of benign and malignant lesions (Fig. 1).

Database

In this study, breast T1-weighted MR images were provided by Vanderbilt University, PI Dr. Thomas E. Yankeelov: QIN-Breast were utilized [35, 36]. This collection contains longitudinal PET/CT and quantitative MR images collected to study treatment assessment in breast cancer in the neoadjuvant

setting. Images were acquired at three-time points: before the start of treatment (t1), after the first cycle of treatment (t2), and either after the second cycle of treatment or after all medicines (before surgery) (t3). The PET/CT images were acquired with a support device built in-house to allow the patient to be in prone to facilitate registration with the MRI data. The value of this collection is to provide clinical imaging data for the development and evaluation of quantitative imaging methods for treatment assessment early in the course of therapy for breast cancer.

The MRI data consist of DWIs, DCE images, and multi-flip data for T1-mapping. The MRIs were obtained using a dedicated 16-channel bilateral breast coil at 3.0T (Philips Achieva with the MammoTrak table). DWIs were acquired with a single-shot spin echo (SE) echo planar imaging (EPI) sequence in three orthogonal diffusion encoding directions (x, y, and z). For 14 patients, b = 0 and 500 s/mm2, TR/TE = 2500 ms/45 ms Δ = 21.4 ms, δ = 10.3 ms and 10 signal acquisitions were acquired. For 19 patients, b = 0 and 600 s/mm2, TR/TE = “shortest” (range = 1800–3083 ms/43–60 ms) Δ = 20.7–29 ms, δ = 11.4–21 ms and 10 signal acquisitions were acquired. For four patients, b = 50 and 600 s/mm2 for two patients), TR/TE = “shortest” (range = 1840–3593 ms/43–60 ms) Δ = 20.6–29 ms, δ = 11.5–21 ms and 10 signal acquisitions were acquired. Before the DCE-MRI acquisition, data for constructing a T1 map were acquired with an RF-spoiled 3D gradient echo multi-flip angle approach with ten flip angles from 2 to 20 degrees in 2o increments. For both the T1 map and DCE scans, TR = 7.9 ms, TE = 4.6 ms, and the acquisition matrix was 192x192x20 (full-breast) over a sagittal square field of view (22 cm^2) with slice thickness of 5 mm. For the DCE study, each 20-slice set was collected in 16 seconds at 25 time points for just under seven minutes of dynamic scanning. A catheter placed within an antecubital vein delivered 0.1 mmol/kg (9–15 mL, depending on patient weight) of gadopentetate dimeglumine, Gd-DTPA, (Magnevist, Wayne, NJ) at 2 mL/sec (followed by a saline flush) via a power injector (Medrad, Warrendale, PA) after the acquisition of the first three dynamic scans (baseline).

Preprocessing

To accurately detect breast cancer, the most critical step is image preprocessing to enhance the breast MR images and reduce the noises of MR imaging instruments and patient movements. The various stages of preprocessing include removing border areas, contrast enhancement, removing noise via filters, etc. In this study, an autoencoder was employed for image preprocessing to reduce noise and extract the saliency features of images.

Convolutional Neural Networks

ResNet was considered as the structure of CNN in this study. According to the literature, the ResNet network is efficient in image analysis and classification. In this model, after input parcellation, the data processing is started. In a Residual block, the input image is processed by a convolution layer, a ReLU layer, and a convolution layer. These transformations produce an F(x) which its output is added to the input of the previous layer. The input data are processed by the modules or passed to the next step without performing any special operations. These networks use stochastic gradient descent instead of

adaptive techniques to prevent interference in the learning process. In this structure, the number of layers increased without any performance reduction.

Experimental Results

All network implementation steps were performed using Matlab software version R2019b on Intel core i7-8700K system with 4.5 GHz processor, 32GB RAM, and Nvidia GTX 1080 Ti Graphic card.

Materials

After selecting the MR images in the middle of the imaging phase to have the entire breast tissue, the images were labeled as positive (1535 malignant) and negative (2565 benign). The initial 16-bit images were converted to 8-bit ones to make calculations more available. After this step, the images were used as inputs of the autoencoder. Autoencoders acted as unsupervised learning via unlabeled data by which the networks reconstruct the outputs that had the minimum differences with 3690 input images. The autoencoder was used as a preprocessing step to provide enhanced images with reduced noises and saliency features. The original images had a slight noise due to electrical waves of an imaging system and patient movement.

In this step, to investigate autoencoder performance in noise reduction, the Gaussian noise with a mean 5 was added to the image by the size of 192×192 for autoencoder training. 90% and 10% of data were used for the training and testing of autoencoder, respectively. Figure 2 represents the autoencoder training using 3690 images along 100 epochs. In this way, the autoencoder achieves desired performance in fast convergence.

A sample of input (noisy) and output (denoise) images of the autoencoder can be seen in Fig. 3 to understand the autoencoder performance. The output reconstructed image with the same size as the input image is accessible with higher contrast and reduced noises.

Besides, the mean squared error (MSE) in Fig. 3 illustrates the differences between the initial image and the Gaussian noisy images (red) as well as between the initial image and the autoencoder output images (blue). The former and latter were represented as Before (red) and After (blue) in Fig. 4. Accordingly, in addition to the significant action of the autoencoder in noise reduction, the output images were reconstructed by salient features that they caused to have images with higher quality in the point of view image analysis and classification.

In the last step and after noise reduction and contrast enhancement by autoencoder, 70% of the preprocessed images for training and 30% for testing were used in CNN defined in the Subsection of Convolutional Neural Networks. This step was repeated for initial images to investigate the autoencoder performance. The results showed the classification of the preprocessed images using autoencoder has higher performance w.r.t the non-preprocessed images. Figure 5 illustrates noisy and denoise images for (a) negative (benign), (b) positive (malignant), which were used as inputs of CNN.

Result Evaluation

To evaluate the performance of the proposed method, the criteria of accuracy, sensitivity, precision, and specificity using Eqs. 1 to 4 were calculated,

$Accuracy = \frac{(TP+TN)}{(TP+TN+FP+FN)}$	(1)
$Sensitivity = \frac{TP}{(TP+FN)}$	(2)
$Precision = \frac{TP}{(TP+FP)}$	(3)
$specificity = \frac{TN}{(FP+TN)}$	(4)

Where TP, TN, FP, and FN are true positive, true negative, false positive, and false negative, respectively. Tables 1 and 2 present the evaluation results of classification implementation with and without autoencoder, respectively.

Table 1 Confusion matrix of Autoencoder+CNN

		Predict Class		
		0	1	
True Class	0	TP=1467	FP=33	97.8%
	1	FN=63	TN=2537	97.57%
		95.88%	98.71%	97.65%

Table 2 Confusion matrix of CNN

True Class \ Predict Class	0	1	
0	TP=1325	FP=174	88.39%
1	FN=247	TN=2354	90.50%
	84.28%	93.12%	89.73%

The performance evaluation results are acceptable in the two examined methods , and the differences in the performance of the two networks are visible. The measured accuracy, sensitivity, precision, specificity, and negative detection rate are 97.65% and 89.73%, 95.88% and 84.28%, 97.8% and 88.39%, 98.71% and 93.12%, as well as 97.57% and 90.50% for the combined autoencoder and CNN and only CNN, respectively.

Discussion And Conclusion

Breast cancer is known as one of the causes of death in women. Correct diagnosis of cancerous tissues based on images and obtaining the size of plaques is essential in treating this disease for the first steps before the disease progresses. There are several methods for diagnosing this type of disease, among which MRI is an extensive clinical method and is an assistant to other methods such as mammography and ultrasound. CAD methods have been widely applied to diagnose lesions on breast MR images; Recently, much attention has been paid to intelligent neural network-based methods in diagnosing the disease. One of these methods is CNN for feature extracting in MR images with a high detection rate. Besides, this fully automated method combined with an autoencoder as a preprocessor creates reliable analysis and classification in MR images.

In the proposed method, the main goal was the diagnosis of benign and malignant breast cancer lesions on MR images with the best performance and high accuracy. For this purpose, the autoencoder network

as a preprocessor to reduce noise combined with CNN has been proposed. The results presented that the autoencoder network can improve CNN performance. In this regard, the accuracy of the CNN network with the autoencoder network in diagnosing this disease was 97.65%. Table 3 summarizes selected studies in the field of breast lesions classification according to their histological type (benign vs. malignant) in breast MRI using DL.

Table 3
Selected studies in the field of breast lesions classification in breast MRI using DL

Method	Result Evaluation	Image Modality	Author(s)
3D ResNet	Acc = 85.5	DCE-MRI	Lou et al., 2019
CNN(VGG)	AUC = 0.88	DCE-MRI	Antropova et al., 2018(a)
3TP-CNN	Acc = 74	DCE-MRI	Gravina et al., 2019
CNN(VGG) + SVM	AUC = 0.65	DCE-MRI	Zhu et al., 2019
CNN(VGG)	AUC = 0.88 ± 0.01	DCE-MRI (T1 and T2 weighted)	Haarburger et al., 2019
MIP + CNN(VGG) + SVM	AUC = 0.88 ± 0.01	DCE-MRI	Antropova et al., 2018(b)
CNN(ResNet34)	AUC = 0.88	DCE-MRI	Truhn et al., 2019
CNN(AlexNet)	Acc = 76	DCE-MRI	Marrone et al., 2017
DenseNet	AUC = 0.811	Ultrafast DCE-MRI	Dalmis et al., 2019
Dense LMST	Acc = 0.847	DCE-MRI + DWI-MRI	Zheng et al., 2018
Cross-Modal DL	Acc = 94	DCE-MRI + mamography	Hadad et al., 2017
CNN(ResNet50)	AUC = 0.97–0.99	DCE-MRI	Zhou et al., 2019
3D CNN	AUC = 0.801	DCE-MRI	Li et al., 2017
Proposed Method (Autoencoder + CNN)	Acc = 97.65	DCE-MRI	Current Study

As shown in Table 3, different methods have been studied and analyzed for feature extraction and benign and malignant tissue classification. The performance of the proposed method is compatible with other DL-based methods for analyzing MR images. The combination of CNN and autoencoder has significantly increased the speed, accuracy, and precision of cancerous tissue classification without manual or semi-automatic segmentation and feature extraction.

Declarations

Conflict of interest

This research did not receive any specific grant from funding agencies in the public, commercial, or not-for-profit sectors.

Ethical approval

This article does not contain any studies with human participants or animals performed by any of the authors.

Informed consent

No new patient data were acquired as part of this work; public data were used from https://wiki.cancerimagingarchive.net/display/Public/QIN-Breast.

References

1. Sites A (2014) SEER cancer statistics review 1975-2011. Bethesda, MD: National Cancer Institute.
2. Huh J, Marmor R, Jiang X (2016) Lessons learned for online health community moderator roles: a mixed-methods study of moderators resigning from WebMD communities. Journal of medical Internet research 18(9):e247.
3. Leunis N, Boumans ML, Kremer B, Din S, Stobberingh E, Kessels AG, Kross KW (2014) Application of an electronic nose in the diagnosis of head and neck cancer. The Laryngoscope 124(6):1377-1381.
4. Morrow M, Waters J, Morris E (2011) MRI for breast cancer screening, diagnosis, and treatment. The Lancet 378(9805):1804-1811.
5. Nachtomy E, Cooperstein R, Vaturi M, Bosak E, Vered Z, Akselrod S (1998) Automatic assessment of cardiac function from short-axis MRI: procedure and clinical evaluation. Magnetic resonance imaging 164:365-376.
6. Fashandi H, Kuling G, Lu Y, Wu H, Martel AL (2019) An investigation of the effect of fat suppression and dimensionality on the accuracy of breast MRI segmentation using u-nets. Medical Physics 46(3):1230–1244.
7. Kuhl C (2007(a)) The current status of breast MR imaging part I. Choice of technique, image interpretation, diagnostic accuracy, and transfer to clinical practice. Radiology 244: 356–378.
8. Kuhl C (2007(b)) Current status of breast MR imaging part 2. Clinical applications. Radiology 244: 672–691.
9. Montemurro F, Martincich L, Sarotto I, Bertotto I, Ponzone R, Cellini L, Redana S, Sismondi P, Aglietta M, Regge D (2007) Relationship between DCE-MRI morphological and functional features and histopathological characteristics of breast cancer. Eur Radiol. 17:1490–1497.
10. Raikhlin A, Curpen B, Warner E, Betel C, Wright B, Jong R (2015) Breast MRI as an adjunct to mammography for breast cancer screening in high-risk patients: retrospective review. AJR Am J

Roentgenol 204:889–897.

11. Rakhlin A, Shvets A, Iglovikov V, Kalinin AA (2018) Deep convolutional neural networks for breast cancer histology image analysis. In International Conference Image Analysis and Recognition. Springer. Cham. 737-744.
12. Platania R, Shams S, Yang S, Zhang J, Lee K, Park SJ (2017) Automated breast cancer diagnosis using deep learning and region of interest detection (bc-droid). In Proceedings of the 8th ACM International Conference on Bioinformatics, Computational Biology, and Health Informatics 536-543.
13. Rasti R, Teshnehlab M, Phung SL (2017) Breast cancer diagnosis in DCE-MRI using mixture ensemble of convolutional neural networks. Pattern Recognition 72:381-90.
14. Yurttakal AH, Erbay H, Ikizceli T, Karaçavus S (2020) Detection of breast cancer via deep convolution neural networks using MRI images. Multimedia Tools and Applications 79(21-22):15555–15573.
15. Amit G, Ben-Ari R, Hadad O, Monovich E, Granot N, Hashoul S (2017) Classification of breast MRI lesions using small-size training sets: Comparison of deep learning approaches. In Proc. Med. Imag., Comput.-Aided Diagnosis 10134:374-379.
16. Antropova N, Huynh BQ, Giger ML (2017) A deep feature fusion methodology for breast cancer diagnosis demonstrated on three imaging modality datasets. Medical Physics 44(10):5162-5171.
17. Drukker K, Edwards A, Papaioannou J, Giger M (2020) Deep learning predicts breast cancer recurrence in analysis of consecutive MRIs acquired during the course of neoadjuvant chemotherapy. Medical Imaging: Computer-Aided Diagnosis. Proc. SPIE 11314, 1131410. doi:10.1117/12.2549044.
18. Fusco R, Granata V, Maio F, Sansone M, Petrillo A (2020) Textural radiomic features and timeintensity curve data analysis by dynamic contrast-enhanced MRI for early prediction of breast cancer therapy response: preliminary data. European Radiology Experimental 4:8. https://doi.org/10.1186/s41747-019-0141-2.
19. Elanthirayan R., Sakeenathul Kubra K., Rajinikanth V., Sri Madhava Raja N., Satapathy S.C. (2021) Extraction of Cancer Section from 2D Breast MRI Slice Using Brain Strom Optimization. In: Satapathy S., Zhang YD., Bhateja V., Majhi R. (eds) Intelligent Data Engineering and Analytics. Advances in Intelligent Systems and Computing, vol 1177. Springer, Singapore. https://doi.org/10.1007/978-981-15-5679-1_71
20. Antropova N, Huynh B, Giger M (2016) SU-D-207B-06: predicting breast cancer malignancy on DCE-MRI data using pre-trained convolutional neural networks. Medical Physics 43(6):3349-3350.
21. Gravina M, Marrone S, Piantadosi G, Sansone M, Sansone C (2019) 3TP-CNN: radiomics and deep learning for lesions classification in DCE-MRI. In Proceedings of the International Conference on Image Analysis and Processing, Springer, Trento, Italy. 661–671.
22. Dalmis M, Gubern-Merida A, Vreemann S, Bult P, Karssemeijer N, Mann R, Teuwen J (2019) Artificial intelligence-based classification of breast lesions imaged with a multiparametric breast MRI protocol with ultrafast DCEMRI, T2, and DWI. Investigate Radiology 54(6):325-332.
23. Truhn D, Schrading S, Haarburger C, Schneider H, Merhof D, Kuhl C (2019) Radiomic versus convolutional neural networks analysis for classification of contrast-enhancing lesions at

multiparametric breast MRI. Radiology 290(2):290–297.

24. Zhu Z, Albadawy E, Saha A, Zhang J, Harowicz MR, Mazurowski MA (2019) Deep learning for identifying radiogenomic associations in breast cancer. Computers in Biology and Medicine 109:85-90.
25. Hu Q, Whitney HM, Giger ML (2019) Transfer learning in 4D for breast cancer diagnosis using dynamic contrast-enhanced magnetic resonance imaging. https://arxiv. org/abs/1911.03022.
26. Hadad O, Bakalo R, Hashoul S, Amit G (2017) Classification of breast lesions using cross-modal deep learning. In Proceedings of the 2017 IEEE 14th International Symposium on Biomedical Imaging (ISBI 2017), Melbourne, Australia. 1:109–112.
27. Antropova N, Abe H, Giger M (2018(a)) Use of clinical MRI maximum intensity projections for improved breast lesion classification with deep convolutional neural networks. Journal of Medical Imaging 5(1): Article ID 014503.
28. Zheng H, Gu Y, Qin Y, Huang X, Yang J, Yang GZ (2018) Small lesion classification in dynamic contrast enhancement MRI for breast cancer early detection. Medical Image Computing and Computer Assisted Intervention—MICCAI2018, Springer, Berlin, Germany. 1:876-884.
29. Antropova N, Huynh B, Li H, Giger ML (2018(b)) Breast lesion classification based on dynamic contrast-enhanced magnetic resonance images sequences with long short-term memory networks. Journal of Medical Imaging 6(1): Article ID 011002.
30. Antropova N, Huynh B, Giger M (2018(c)) Recurrent neural networks for breast lesion classification based on DCEMRIs. In Proceedings of the SPIE Medical Imaging 2018: Computer-Aided Diagnosis. 10575, Article ID UNSP10575M, Houston, TX, USA, February.
31. Li J, Fan M, Zhang J, Li L (2017) Discriminating between benign and malignant breast tumors using 3D convolutional neural network in dynamic contrast enhanced-MR images. In Proceedings of the Medical Imaging 2017: Imaging Informatics for Healthcare, Research, and Applications. 10138, Article ID UNSP1013808.
32. Haarburger C, Baumgartner M, Truhn D, Broeckmann M, Schneider H, Schrading S, Kuhl C, Merhof D (2019) Multi scale curriculum CNN for context-aware breast MRI malignancy classification. In Proceedings of the International Conference on Medical Image Computing and Computer-Assisted Intervention, Springer, Shenzhen, China. 495-503.
33. Luo L, Chen H, Wang X, Dou Q, Lin H, Zhou J, Li G, Heng P (2019) Deep angular embedding and feature correlation attention for breast MRI cancer analysis. In Proceedings of the International Conference on Medical Image Computing and Computer-Assisted Intervention, Springer, Shenzhen, China. 504-512.
34. Zhou J, Luo LY, Dou Q, Chen H, Chen C, Li G, Jiang Z, Heng P (2019) Weakly supervised 3D deep learning for breast cancer classification and localization of the lesions in MR images. Journal of Magnetic Resonance Imaging 50(4):1144-1151.
35. Li X, Abramson RG, Arlinghaus LR, Kang H, Chakravarthy AB, Abramson VG, Farley J, Mayer IA, Kelley MC, Meszoely IM, Means-Powell J, Grau AM, Sanders M, Yankeelov TE (2015) Multiparametric

magnetic resonance imaging for predicting pathological response after the first cycle of neoadjuvant chemotherapy in breast cancer. Investigative Radiology 50(4):195-204. PMCID: PMC4471951.

36. Li X, Abramson RG, Arlinghaus LR, Chakravarthy AB, Abramson VG, Sanders M, Yankeelov TE (2016) Data from QIN-Breast. The Cancer Imaging Archive.

Figures

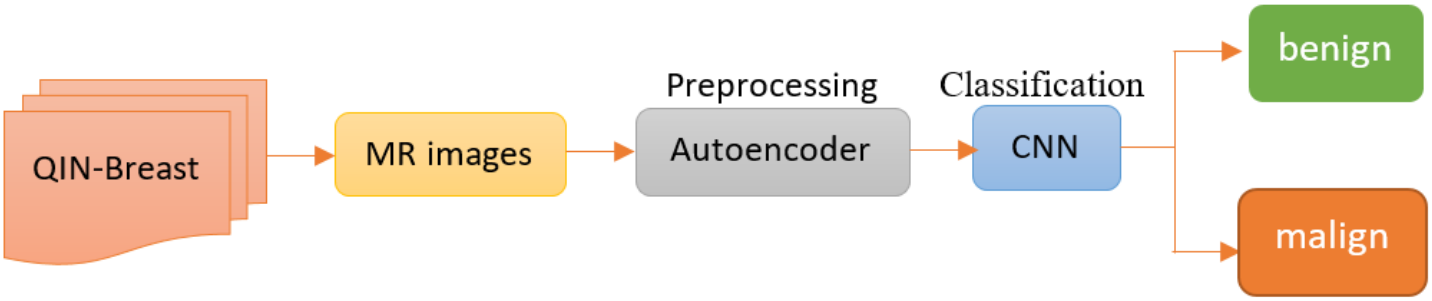

Figure 1

Block diagram of the proposed method

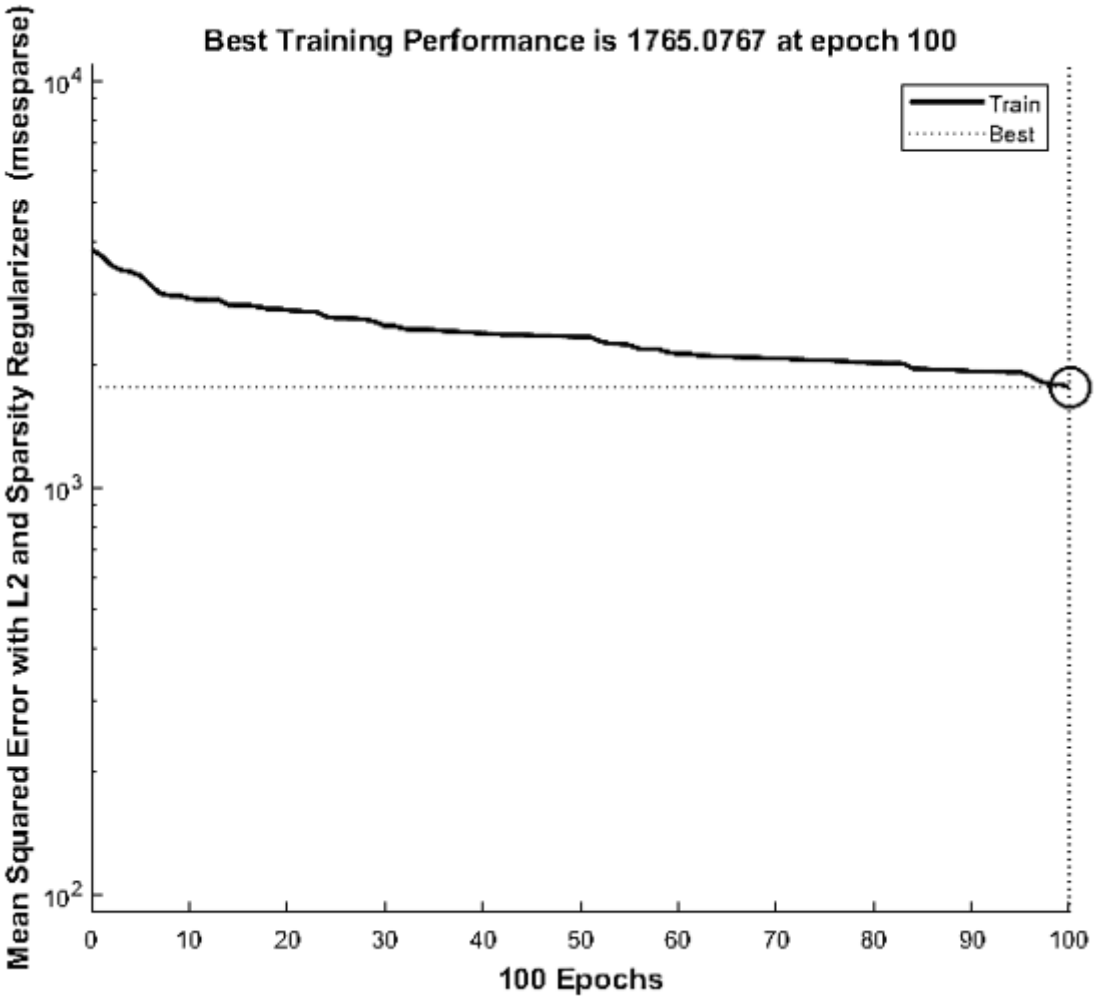

Figure 2

Autoencoder training using 3690 images

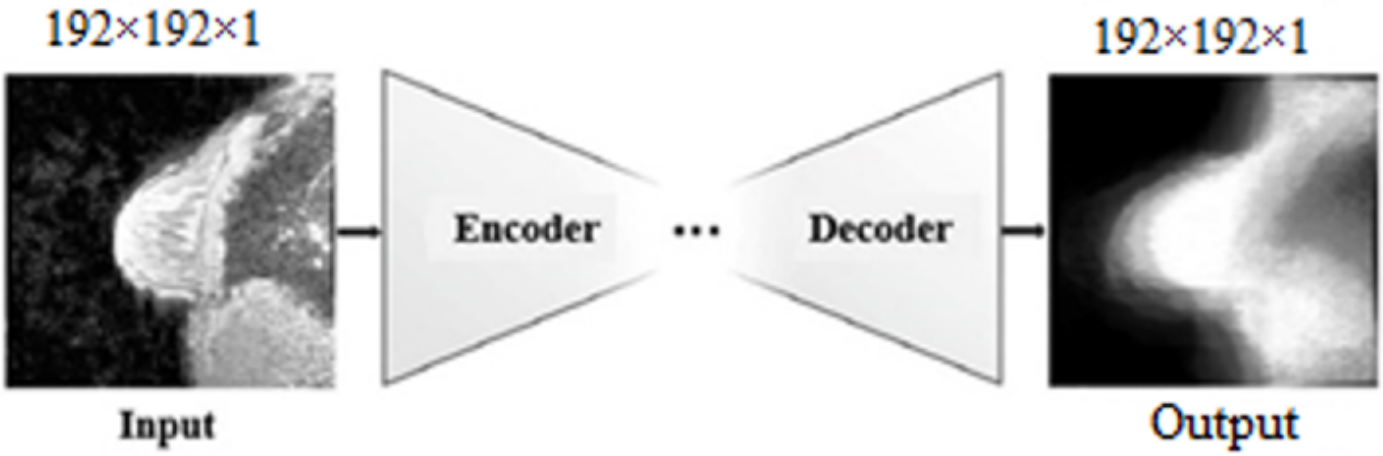

Figure 3

A sample of input (noisy) and output (denoise) images of the autoencoder.

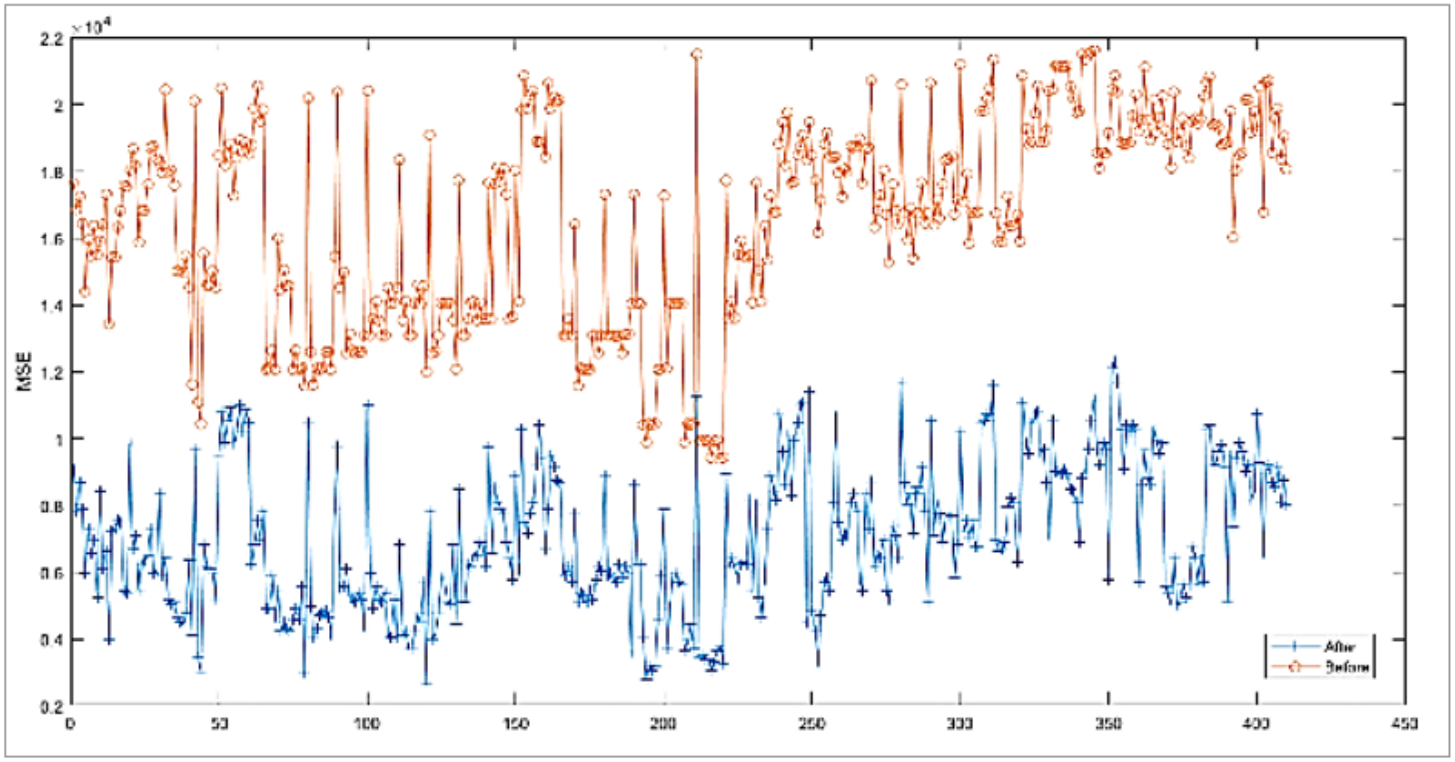

Figure 4

MSE between the initial image and the Gaussian noisy images (Before in red), MSE between the initial image and the autoencoder output images (After in blue).

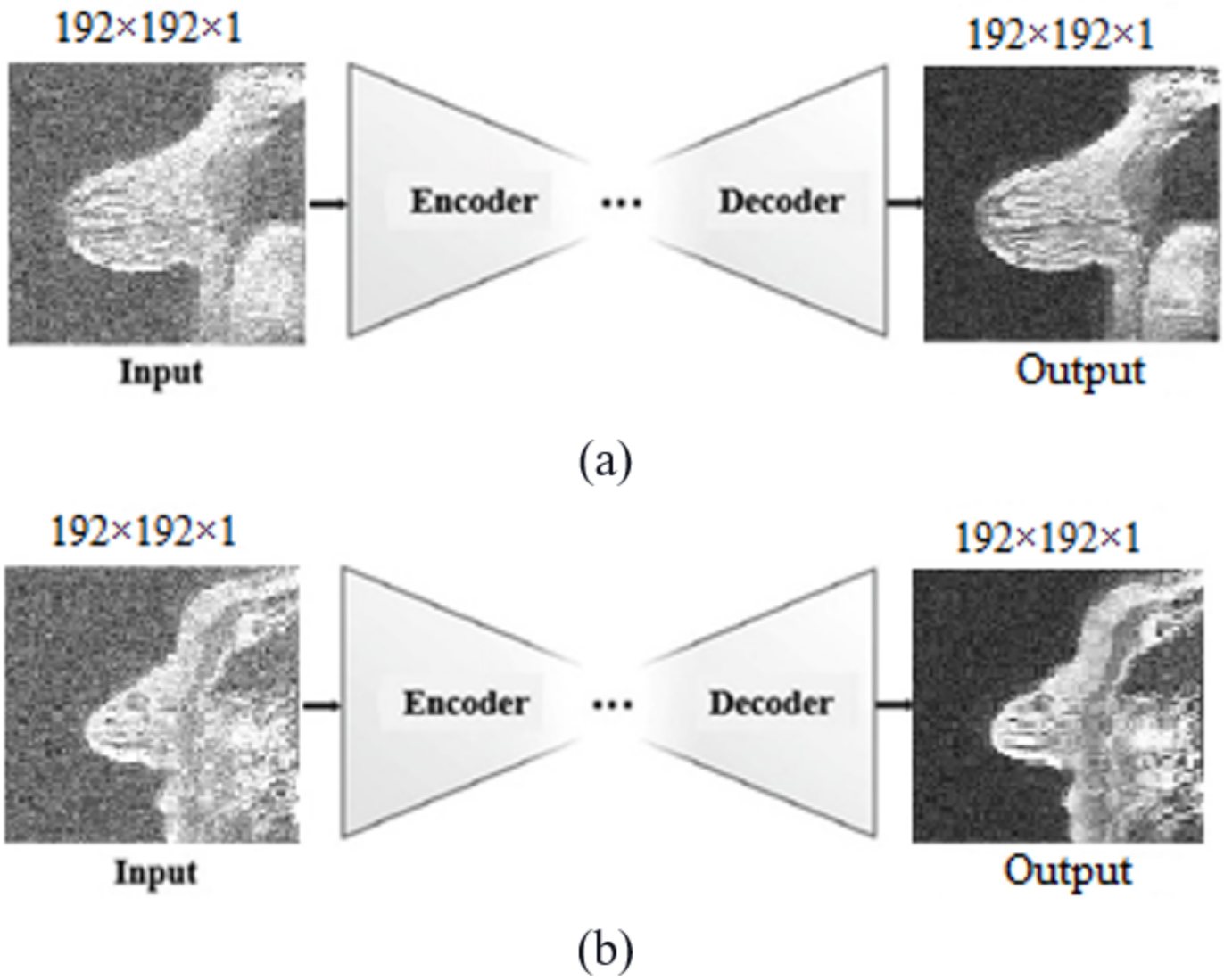

Figure 5

Input and output of autoencoder as noisy and denoise images for (a) negative (benign), (b) positive (malignant).